Experimental Eye Research 234 (2023) 109566

Contents lists available at ScienceDirect

Experimental Eye Research

journal homepage: www.elsevier.com/locate/yexer

Research article

Retinal vascular remodeling in photoreceptor degenerative disease

Matthew Nguyen, James Sullivan, Wen Shen *

Department of Biomedical Science, Charles E. Schmidt College of Medicine, Florida Atlantic University, Boca Raton, FL, USA

ARTICLE INFO

Keywords:
Retinal degeneration
Retinal vasculature
Vascular degeneration

ABSTRACT

Abnormal vasculature in the retina, specifically tortuous vessels and capillary degeneration, is common in many of the most prevalent retinal degenerative diseases, currently affecting millions of people across the world. However, the formation and development of abnormal vasculature in the context of retinal degenerative diseases are still poorly understood. The FVB/N (rd1) and rd10 mice are well-studied animal models of retinal degenerative diseases, but how photoreceptor degeneration leads to vascular abnormality in the diseases remains to be elucidated. Here, we used advancements in confocal microscopy, immunohistochemistry, and image analysis software to systematically characterize the pathological vasculature in the FVB/N (rd1) and rd10 mice, known as a chronic, rapid and slower retinal degenerative model, respectively. We demonstrated that there was plexus-specific vascular degeneration in the retinal trilaminar vascular network paralleled to photoreceptor degeneration in the diseased retinas. We also quantitatively analyzed the vascular structural architecture in the wild-type and diseased retinas to provide valuable information on vascular remodeling in retinal degenerative disease.

1. Introduction

The vascular and nervous systems, two major networks in the mammalian retina, exhibit a high degree of anatomical parallelism and functional crosstalk. During retinal development, neuronal and glial progenitors and mature cells guide and attract blood vessels to form a trilaminar vascular network that supports the high metabolic needs of the neural tissues. In general, there are two arterial inputs to the eye: the posterior ciliary arteries that only supply the choroid and the central retinal artery. The main source of the retinal blood supply originates from the central retinal artery that branches into several retinal arterioles radiating towards the retinal periphery to connect retinal venules that form the superficial vascular plexus in the nerve fiber layer. The retinal arterioles further branch into precapillary arterioles, which give rise to a capillary network forming the intermediate and deep vascular plexus lining each side of the inner nuclear layer (Ivanova et al., 2014; Selvam et al., 2018). Together with the superficial plexus (SP), the trilaminar vascular network brings oxygen and nutrients to the inner and outer retina, supporting retinal development, metabolism, and homeostasis. Importantly, any deviations from normal vascular organization and proliferation can have grave consequences for the function of the retina. It has been documented that a disruption of vasculature is one of the pathological changes common to retinal degenerative diseases (Sun and Smith, 2018; Ferna´ndez-S´anchez et al., 2018); however, it is still unclear how disease onset and progression lead to pathological changes in the retinal vasculature.

The major inherited retinal degenerative diseases, e.g., retinitis pigmentosa (RP), have a high incidence of blindness affecting people of all ages, including infants. RP typically begins with the loss of rod photoreceptors because of a genetic mutation, followed by cone degeneration in the retina. Without these cells the phototransduction cascade, a molecular signaling pathway that involves the detection and conversion of light stimuli into nerve signals, is not possible. Therefore, progressive vision loss is often seen in degrading into total blindness. Given the severity and impact of these diseases, more information on pathologies, especially the vascular pathology of RP, is urgently required. While in humans it is difficult to visualize changes in retinal vascular development due to the prenatal nature, the development of retinal vasculature in mice is a postnatal process involving layer-by-layer formation of a trilaminar vascular network, which can be easily visualized and detected through microscopy and an imaging system. During mouse retinal development, the trilaminar vascular network branches off of the central retinal artery after birth, and then makes up the SP, intermediate plexus (IP), and deep plexus (DP) within two weeks

Abbreviations: SP, Superficial plexus; IP, Intermediate plexus; DP, Deep plexus; INL, Inner nuclear layer; RP, Retinitis Pigmentosa; rd mouse, Rod photoreceptor degenerative mouse model.

* Corresponding author.
E-mail address: wshen@health.fau.edu (W. Shen).

https://doi.org/10.1016/j.exer.2023.109566
Received 1 March 2023; Received in revised form 5 June 2023; Accepted 3 July 2023
Available online 7 July 2023

after birth. Vascular development is complete in the third postnatal week (Milde et al., 2013). Thus, the postnatal development allows us to track vascular growth, changes, and remodeling in inherited retinal degenerative diseases.

The mouse retina is an excellent model for studying neurodegeneration-induced pathological changes of vasculature since there are various genetic models for retinal degeneration available (Chang et al., 2002). The RP mouse models, rd1 and rd10 mice, have proven to be relatively well-studied animal models. Both rd1 and rd10 mice carry a mutation in the *pde6b* gene, which faultily encodes the β subunit of cGMP phosphodiesterase (PDE) in rod photoreceptors, leading to severe retinal degeneration (Bowes et al., 1990; Chang et al., 2002). Indeed, mutations in the gene encoding the β subunit of cGMP-PDE have been found in human patients suffering from autosomal recessive RP. The rd1 and rd10 are two similar mouse models, but with different time frames of photoreceptor degeneration. The rd1 mice are characterized as a fast model of retinal degeneration, typically losing rod photoreceptors within two weeks of birth, which profoundly affects the gradual maturation of cone photoreceptors during retinal development (Carter-Dawson et al., 1978; Yang et al., 2015). Conversely, photoreceptor degeneration in the rd10 mouse does not typically occur until after the fourth postnatal week when vascular development is essentially complete, which has been considered as a slower degeneration model (Barhoum et al., 2008; Phillips et al., 2010; Li et al., 2019). We used these two mouse models to assess and characterize the pathological changes of retinal vasculature in response to rapid and slower photoreceptor degeneration that respectively occur in the premature and adult RP mice retinas.

In this study, we showed that photoreceptor degeneration can cause severe capillary loss in the DP of the retina in both rd1 and rd10 mice. The results suggest that the loss of capillary microcirculation creating hypoxic conditions in the distal retinas, may contribute to the acceleration of photoreceptor degeneration in the RP retinas. Additionally, we found that rapid photoreceptor degeneration in the rd1 retina suppresses vascular development in the distal retina, correlating at least in part, with the suppression of cadherin protein expression in the endothelium cells. We analyzed the trilaminar vascular structure and the growth and remodeling of vessels from development to adulthood, providing detailed information for retinal vascular remodeling in the RP animal models. Such detailed knowledge is important as disease-specific mechanisms often affect the retinal vasculature in a plexus-specific manner. In conclusion, our results indicate that retinal vascular growth and maintenance largely depend on the function of photoreceptors that play a critical role in neurovascular coupling in the distal retina.

2. Materials and methods

All described procedures involving live animals were approved by the Institutional Animal Care and Use Committee of Florida Atlantic University. The study was conducted in compliance with federal regulations and the ARVO Statement for the Use of Animals in Ophthalmic and Vision Research.

2.1. Animals

The FVB/N (rd1, pde6b) with a 129 SvEv background, rd10 (B6.CXB1-pde6brd10/J) with a C57BL/6 background, and wild-type 129SvEv and C57BL/6 mice were purchased from the Jackson Laboratory and bred in house to produce the offspring for the study. FVB/N and wild-type 129SvEv mice were kept in the animal facility under a 12-h dark/light cycle. The illumination levels in the mouse housing room were approximately 200 Lux. FVB/N mice are severely visually impaired due to a homozygous null mutation in the retinal degeneration 1 allele *Pde6b*^{rd1} encoding the catalytic β subunit of the phosphodiesterase 6 (PDE6β) protein that is essential for the proper function of rod phototransduction. The mutation results in blindness by the weaning age.

For the rd10 and wild-type C57BL/6 control mice, the light cycle for breeder pairs was set at a 12-h dark/dim light cycle. Once pups were born, the cages were transferred to 24-h constant darkness, with only a dim red light being used for husbandry duties (i.e., 15 min health checks daily and 1 h cage change per week) to mimic dark conditions (cf. Cronin et al., 2012). The rd10 is a spontaneous missense point mutation in *Pde6b*. Although similar to the rd1, the rd10 phenotype has a later onset and milder retinal degeneration by weaning age. The dark-rearing the mice from birth can protect photoreceptor degeneration and extended the therapeutic window for the rd10 (Chang et al., 2007; Pang et al., 2008).

The mice used in the histological and immunohistochemical experiments were euthanized by intraperitoneal injection of a mixture of ketamine (200 mg/kg) and xylazine (10 mg/kg) followed by the cervical dislocation procedure.

2.2. Immunohistochemical and histological labeling

Freshly enucleated eyes were fixed for 20 min in a phosphate-buffered saline (PBS) solution containing 4% paraformaldehyde. After removing the cornea and lens, retinal tissues were removed from the eyecups and placed in the fixative for another 15 min, washed in a PBS solution 3 times, rinsed with PBS plus 0.1% Tween and 0.3% Triton (PBST-T), and then treated with a blocking solution consisting of 10% normal goat or donkey serum in PBST-T. They were then incubated in primary antibodies: anti-CD31 and anti-CD144, in a 1:2000 dilution for 3 days at 4 °C. After three 15min washes with PBST-T, the retinas were incubated in a fluorescent conjugated secondary antibody: either Alexa 488 or Cy-3 (Jackson Immunoresearch, West Grove, PA), at a concentration of 1:2000, overnight at 4 °C. The retinas were subsequently rinsed with PBST-T solution, mounted in Vectashield mounting medium (Vector Laboratories, Burlingame, CA), and viewed with a confocal laser-scanning microscope (LMS 700, Zeiss, Munich, Germany). Images were acquired with 20x and 40× objectives and processed with the Zeiss Microscope Software Zen.

For hematoxylin and eosin (H&E) histology, following fixation, the eyecups were rinsed in PBS solution, dehydrated in graded sucrose solutions (10%, 15%, 20%, and 30%), and immersed in 30% sucrose overnight at 4 °C. The dehydrated eyecups were embedded in OCT compound (Ted Pella, Redding, CA), frozen overnight, and then sectioned at 8–10 μm on a cryostat. The cryostat sections were collected on slides, air dried, and stored at −80 °C. The cryostat sections were stained with the H&E staining kit (Vector Laboratories, Burlingame, CA), following the manufacture's recommended procedure. Briefly, the cryostat sections were rehydrated with distilled water. Then, the sections were completely covered by the hematoxylin solution, incubated for 5 min, and rinsed with distilled water 3 times to remove the excess staining; the sections were treated with the bluing reagent for 10–15 s and rinsed in distilled water 3 times before 100% ethanol was applied, covering the tissue sections for 10–20 s. Then, the Eosin Y solution was applied and the sections were incubated for 2–3 min, followed by rinsing the sections with 100% ethanol and dehydrating the tissue sections in the ethanol solution for 2 min. The H&E-stained tissue sections were covered with glass coverslips and viewed with a Nikon Eclipse microscope (Nikon, Japan). The images were processed with the Nikon NIS Elements software.

2.3. Confocal imaging and data analyses

Confocal z-stack images with vertical sectioning in a 0.5 or 1 μm step resolution were acquired in each vascular plexus in whole-mount retinas. The images were acquired in the central, middle, and peripheral areas of the dorsal, ventral, nasal, and temporal retina. Some lower-magnification images were only acquired in central and peripheral

areas of the retina. These enabled us to assess the vascular layers and detect temporal and structural differences in the vasculature in the diseased retinas as compared to the control retinas. The original images were processed and converted into binary images using the ImageJ (FIJI) software to isolate blood vessels from the background. Vascular densities in each singular plexus were analyzed using the vascular area percentage, which is also called area fraction, that is the ratio of fluorescent-labeled area for blood vessels to total retinal area of 640 μm^2. The quantity of vascular branches and vessel lengths in the DP were analyzed per 640 μm^2, and the quantity of vessel sprouts in the SP were manually counted per 640 μm^2 in the central, middle, and peripheral areas of the retinas. The percentages of vessel radial outgrowth were calculated by dividing the retinal area covered by blood vessels by the total retinal area. Data were assessed quantitatively and expressed as mean ± standard error of the mean (SEM) with n representing the number of images averaged from 3 to 4 retinas.

3. Results

3.1. Progression of photoreceptor degeneration in FVB/N and rd10 mouse retinas

The FVB/N mouse contains a naturally occurring *pde6b* gene mutation (homozygous for the rd1 mutation) that causes rapid rod photoreceptor degeneration, resulting in blindness by weaning age (Gimenez and Montoliu, 2001). Retinal sections were prepared from the FVB/N mice at postnatal (P) days of P7, P14, P21, and 1 month, from neonates to early adulthood. The age-dependent retinal structural changes of the FVB/N were shown via H&E staining (Fig. 1A). By P14, the FVB/N retina was thinner than normal due to the loss of a substantial number of photoreceptors in the outer nuclear layer (ONL). A severe decline of photoreceptors was seen at P21 along with even greater retinal thinning, leading ultimately to the loss of the ONL, as seen at 1 month age of the FVB/N retina. By contrast, there was robust staining of photoreceptor

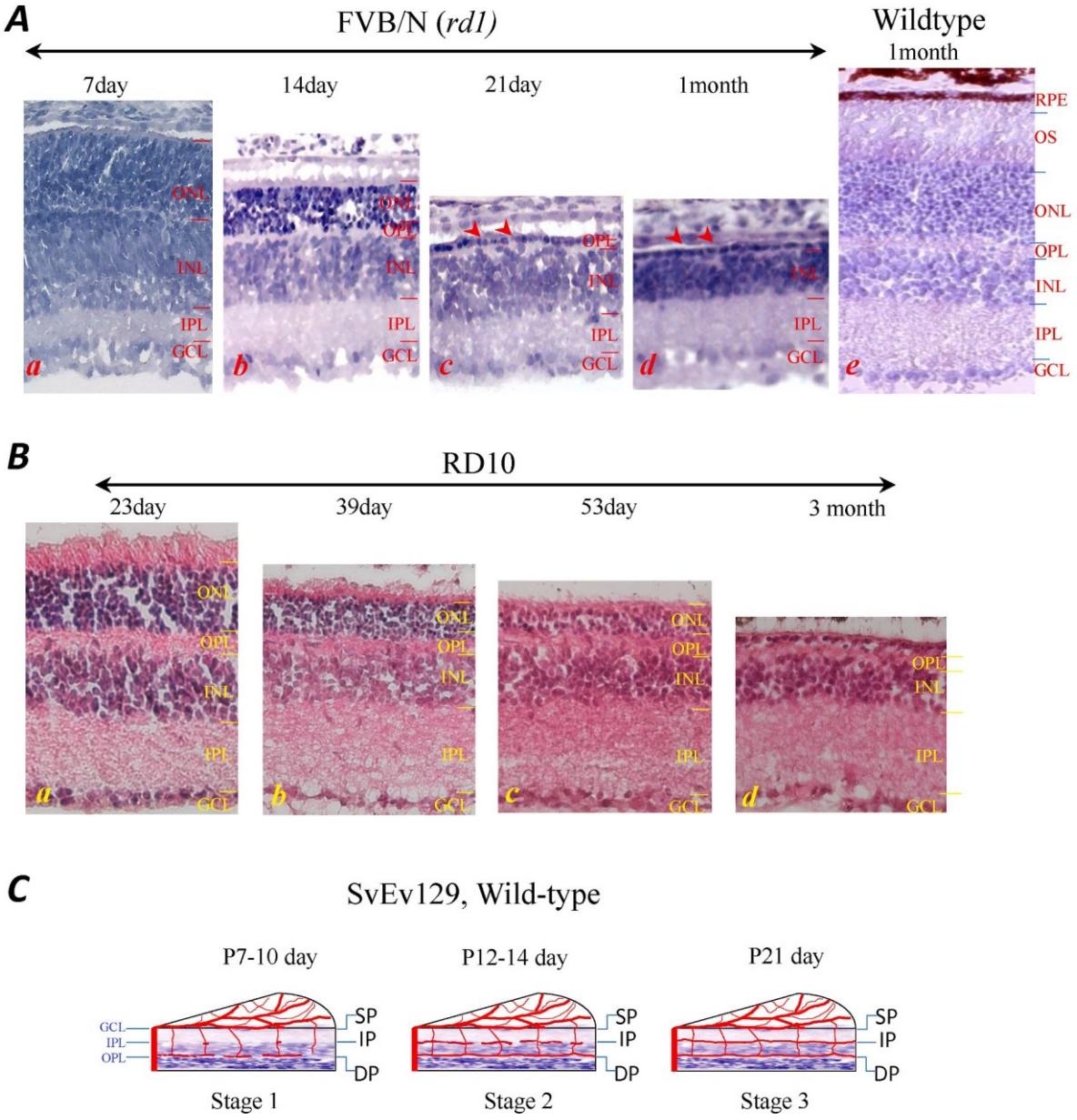

Fig. 1. Progressive photoreceptor degeneration and loss of the outer nuclear layer (ONL) in the retinas of the FVB/N (rd1) mice at various ages; the wild-type 129SvEv served as a control (A). Age-dependent photoreceptor degeneration in the retinas of rd10 mice (B). (C) Schematics of retinal vascular development stages of the wild-type 129SvEv mouse retina.

nucleus in the ONL of the wild-type control retina (see *e* in Fig. 1A), and the thickness of the inner nuclear layer (INL) and the ganglion cell layer (GCL) appeared to be far less affected by the degenerative changes taking place in the distal retina in this time frame. The FVB/N retina typically exhibits rapid photoreceptor degeneration within the period of retinal development. The histological results are consistent with our earlier findings from antibody labeling experiments (Yang et al., 2015).

As compared with the FVB/N retina, photoreceptor degeneration was not noticeable in the rd10 retina during retinal development from P1 to P21. H&E staining shows that most photoreceptors were present in the rd10 retina at P23, as indicated in the thickness of the ONL (see *a* in Fig. 1B). The rd10 mice usually undergo progressive photoreceptor degeneration after P23 when the retinal development is complete (Li et al., 2019). Significant photoreceptor degeneration and a decline in the thickness of the ONL were seen at P39 and P53 (see *b* and *c* in Fig. 1B), the stages in which the animals lose vision. The time-dependent changes

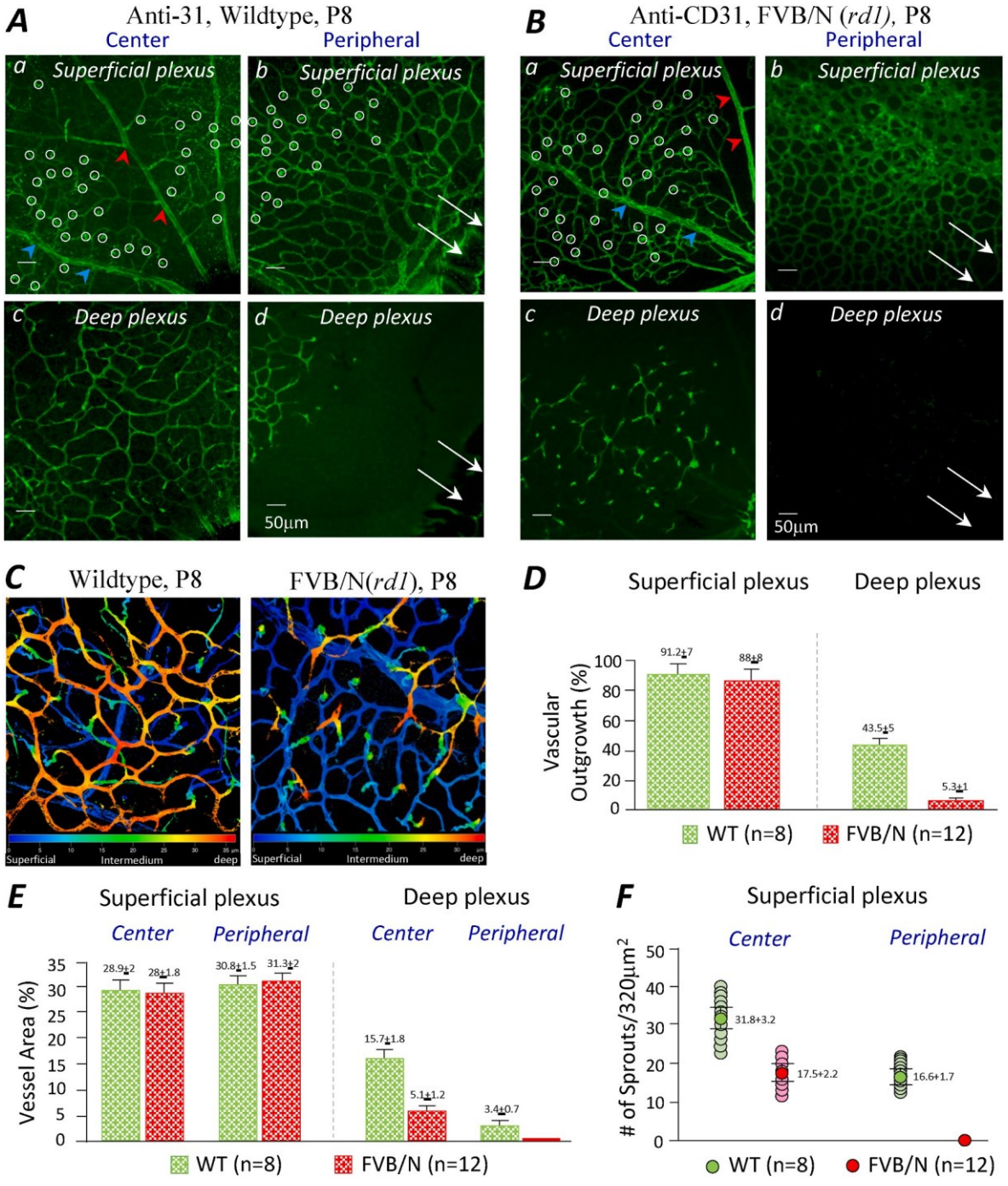

Fig. 2. Retinal vascular development in the wild-type and FVB/N mouse at P8. Confocal z-stack images on whole-mounted retinas were labeled with the blood vessel marker anti-CD31, showing vascular development in the superficial and deep plexus of the wild-type 129SvEv (A) and FVB/N mouse retinas (B). An arteriole and a venule in the superficial plexus are indicated by red and blue arrowheads, respectively; the white arrows point at the retinal periphery and the vascular sprouts are marked by white circles. (C) Z-stack depth color coding images showing the suppression of vascular development in the deep plexus of the FVB/N retina. Quantification and comparison of vascular outgrowth, vascular density, and the number of sprouts in the central and peripheral areas of the superficial and deep plexus of the wild-type and FVB/N retina (D, E, F). (bar: 50 μm). (For interpretation of the references to color in this figure legend, the reader is referred to the Web version of this article.)

of retinal structure confirmed that the rd10 mouse represents a slower degenerative RP model.

3.2. Vascular development in the wild-type 129SvEv mouse retina

The growth of mouse retinal vessels shortly after birth follows a stereotyped architecture composed of three parallel vascular plexuses, which is referred to as the trilaminar vascular network. Fig. 1C illustrates the retinal vascular development in wild-type 129SvEv, specifically, the formation of each plexus of the trilaminar network in a time-specific manner within three stages. The initial formation of the SP in the nerve fiber layer occurred within the first 10 days after birth. Vessels from the SP then infiltrated below the inner nuclear layer (INL) and began the process of forming the DP in the distal retina, typically between P4 to P10. Around P12, vessels began to form the IP on the surface of the INL in the inner retina. We also observed that the extension of the trilaminar plexuses from the central retina to the middle and peripheral regions was typically completed after the second postnatal week. Our results regarding the temporal and spatial development of the retina vasculature in the129SvEv strain are similar to those reported in previous studies in different mouse strains (Milde et al., 2013; Chen et al., 2016).

3.3. Influence of early-onset photoreceptor degeneration on vascular development

Confocal images were acquired in the retinas of the wild-type 129SvEv and FVB/N mice at p8, p14, and p21: the critical time points for retinal vascular development concomitant with rapid photoreceptor degeneration in the diseased retina. Blood vessels in the retinas were labeled with the antibody targeting the platelet endothelial cell adhesion molecule (PECAM1), also known as CD31, which is highly expressed on the surface of endothelial cells of retinal arterioles, venules, and capillaries (DiMaio et al., 2008). Indeed, the antibody for CD31 (anti-CD31) is a widely accepted marker for detecting the formation, differentiation, and density of vasculature. Fig. 2A shows a set of confocal z-stack images of anti-CD31-labeled retinal blood vessels of the wild-type mice at P8 that were acquired in central and peripheral areas of the retina. Because the anti-CD31-labeled arterioles and venules can be distinguished from each other, the images depict the formation of the SP with branched arterioles (red arrowheads), unbranched venules (blue arrowheads), and capillary beds (see *a* Fig. 2A), as well as the outgrowth of the vessels towards the retinal periphery (see the white arrows in Fig. 2A), evidencing that the rapid formation of the SP occurred in the first week of birth. At P8, vertical sprouting from the venules and capillary bed (see white circles) are seen to be growing towards the distal retina to form the DP in the outer boundary of the INL. The newly formed DP is shown in Fig. 2A*c* &2Ad. The capillary meshwork covered the central and middle area, but not peripheral areas of the DP, corresponding to the vascular sprouting pattern in the SP. The results indicate that the vascular outgrowth in the DP follows the same center-to-periphery pattern to that seen in the SP during retinal development.

In the age-matched FVB/N retina, the anti-CD31-labeled SP showed that the primary arterioles and venules were oriented radially from the retinal center to the periphery (see the red and blue arrowheads, Fig. 2B*a* & 2Bb). The SP of the FVB/N retina appears relatively normal compared to the wild-type control. However, the vessel sprouting only occurred in the central area of the retina, approximately 150 μm from the optic nerve head. Interestingly, most of the vessel sprouts arose from venules and their capillaries, but not arterioles in the SP (see the white circles, Fig. 2B*a*). In addition, only a few new capillaries formed in the central area of the DP, and no capillaries formed in the peripheral area of the DP (Fig. 2B*c* & 2Bd) at this age. The differences between the wild-type and FVB/N mice in vascular development are illustrated in the 2C projection images with depth coding from the SP (blue color) to DP (red color), which were acquired in the central areas of the retinas (Fig. 2C). The findings indicate that DP development in the FVB/N retina was suppressed as early as in the first week of retinal development.

To quantitatively analyze the abnormal vascular development in the FVB/N retina at P8, we calculated the anti-CD31-labeled vessel area fraction (ratio of area covered by blood vessels to the total retinal area), vascular outgrowth, and the quantity of sprouting vessels of the SP and DP, as compared with those of the wild-type control. The histograms in Fig. 2D indicate the average vascular outgrowth (%) in the SP and DP of the wild-type and FVB/N retina, showing 91.2 ± 7% (n = 8) and 88 ± 8% (n = 12) outgrowth in the SP of the wild-type and FVB/N retinas, respectively, and 43.5 ± 5% (n = 8) and 5.3 ± 1% (n = 12) outgrowth in the DP of the wild-type and FVB/N retinas, respectively. Comparing the average quantities from wild-type and FVB/N retinas, there were approximately 3.5% and 87.8% reductions in vascular outgrowth in the SP and DP of the FVB/N retinas, respectively, indicating that the capillary network in the DP was undeveloped in the diseased retina at P8.

The average vessel area fractions (%) of the SP in the central and peripheral retina were 28.9 ± 2 and 30.8 ± 1.5 (n = 8) for the wild-type and 28 ± 1.8 and 31.3 ± 2 (n = 12) from the FVB/N, respectively, confirming that the early-onset photoreceptor degeneration had no significant effects on SP development in the FVB/N retina (Fig. 2E, left). However, the vessel area fractions of the DP in the central and periphery were largely reduced, i.e., 5.1 ± 1.2 and 0 (n = 12) in the FVB/N retinas compared to 15.7 ± 1.8 and 3.4 ± 0.7 (n = 8) in the wild-type retinas (Fig. 2E, right).

The quantity of vessel sprouts was calculated on the SP of both the wild-type and FVB/N retinas, as shown in Fig. 2F. The average numbers of vessel sprout per 320 μm^2 were 31.8 ± 3.2 (n = 8, central area) and 16.6 ± 1.7 (n = 8, peripheral area) in the wild type, while in the FVB/N retina, the numbers were 17.5 ± 2.2 (n = 12, central area) and 0 (n = 12, peripheral area). The results indicate that early-onset photoreceptor degeneration suppresses the vessels sprouting from the SP, leading to impaired DP development in the retina. The abnormal vascular development in the diseased retina could be detected as early as P8.

3.4. Suppression of vascular endothelial (VE)-cadherin protein expression in the FVB/N mouse retina detected at P8

VE-cadherin, a major component of vascular endothelial adherent junctions, is an important endothelial protein required for vascular formation and maintenance (Bravi et al., 2014). We found that VE-cadherin expression in the formation of the DP was suppressed in early-onset photoreceptor degeneration. VE-cadherin is also known as CD144. The specific antibody for CD144 (anti-CD144) was used to detect protein expression in retinal vascular development at P8. The confocal images, acquired in the central and peripheral retina, show the anti-CD144-labeled SP and DP of the wild-type retina (Fig. 3A). Apparently, VE-cadherin proteins are expressed in both the SP and DP, and on the vertical spouting vessels (see the white circles). Cross-section views along the z-axial further show the anti-CD144-labeled vessels infiltrating vertically from the SP to the DP, and crossing the INL in the central and peripheral areas of the wild-type retina (see Fig. 3A*e* and 3A*f*).

The anti-CD144-labeled age-matched FVB/N retina exhibited normal arterioles (red arrowheads), venules (blue arrowheads), and capillary beds in the SP (Fig. 3B*a*); however, no CD144 labeling was detected in the DP of the retina (Fig. 3B*b*). The cross-section views show that CD144 labeling was only present in a few spouting vessels, but not in the DP of the retina (Fig. 3B*c* and 3Bd). A lack of VE-cadherin in the distal retina could be one of the causes of impaired DP formation in the FVB/N mouse retina.

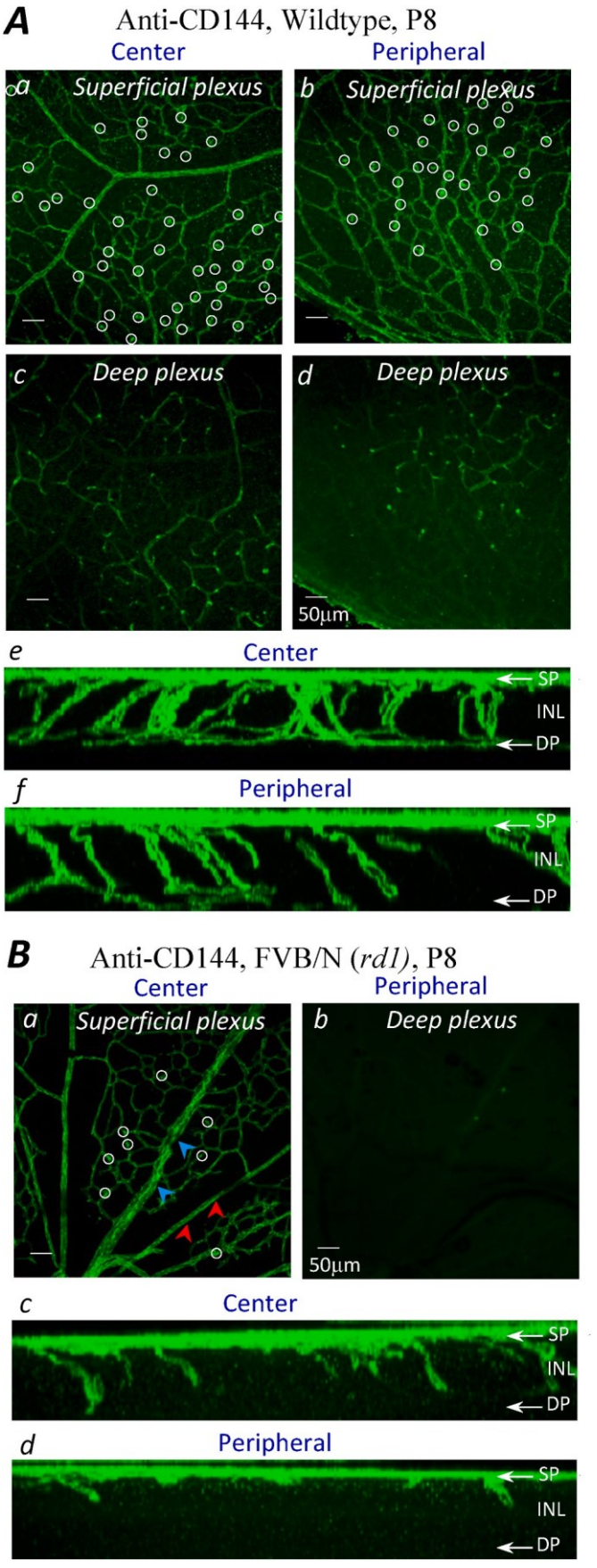

(caption on next column)

Fig. 3. The absence of VE-cadherin (CD144) protein expression in the development of the deep plexus in the FBV/N mouse retina at P8. (**A**) VE-cadherin proteins present in the superficial plexus (SP) and deep plexus (DP) of the wild-type retina in a flat-mount (*a-d*) and cross-section (*e*), viewed in confocal z-stack projection images. (**B**) VE-cadherin is present in the superficial plexus but absent in the deep plexus of the FVB/N retina. (bar: 50 µm). **INL**: Inner nuclear layer. Image stacks with high z-resolution (0.5 mm) projected into one image. White circles: vessel sprouts. Red arrowheads: arteriole. Blue arrowhead: venule. (For interpretation of the references to color in this figure legend, the reader is referred to the Web version of this article.)

3.5. Vascular remodeling in the FVB/N retina detected at P14

At P14, the time at which the IP begins to form in the inner retina of wild-type mice; both wild-type and FVB/N retinas were labeled with anti-CD31. Then, confocal z-stack images were acquired on each vascular plexus of the trilaminar network. Fig. 4A shows a set of representative images from the wild-type retina at P14. As can be seen, large arterioles, venules, and a capillary bed are present in the SP (see *a, e, i* in Fig. 4A) and the capillary meshwork is present in the DP (see *c, g, k* in Fig. 4A) of the central, middle, and peripheral retina. This demonstrates that SP and DP vascular development was nearly complete at this age, while the vascular network in the IP was still developing, as indicated by the anti-CD31-labeled sparse capillary tunica (see *b, f, j* in Fig. 4A). Cross-sectional views along the z-axial depict the trilaminar vascular structure labeled with anti-CD31, showing a strongly labeled SP and DP and a weakly labeled IP (see *d, h, l* in Fig. 4A), evidencing a lower density of capillaries in the IP.

Significant vascular remodeling was seen in the age-matched FVB/N retina. Only a few dilated vessels were present in the DP at P14 (Fig. 4B*c*). Interestingly, a highly dense capillary network formed in the IP (Fig. 4B*b*), although the SP seemed to have formed normally (Fig. 4B*a*). A cross-sectional view of the trilaminar network further confirmed that anti-CD31 was observed extensively in the SP and IP, and only a few vessel branches ascended from the SP to the DP (Fig. 4B*d*).

The changes in vascular density in each plexus were quantitatively analyzed and compared with the average vascular area fractions (%) of the wild-type and FVB/N retinas. The results are shown in Fig. 4C. They indicate that at P14, the average vascular area fractions of the SP (central, middle, and peripheral retina) were 31.2 ± 2, 28.4 ± 1.8, and 27.2 ± 1.5 (n = 8) in the wild-type and 30.7 ± 2.1, 30 ± 2.4, and 28 ± 1.4 (n = 8) in the FVB/N retina (Fig. 4C, left panel). The results indicate that vascular development in the SP was not affected by the rapid photoreceptor degeneration observed in the second postnatal week. However, the average vascular area fractions were noticeably increased in the IP of the FVB/N retina, i.e., 13.7 ± 1, 15.9 ± 1.5, and 7.1 ± 1 (n = 8) in the wild-type increased to 23.5 ± 1.8, 25.8 ± 1.5, and 22.5 ± 1.2 (n = 8) in the FVB/N retina (Fig. 4C, middle panel). The quantitative data also exhibited a significant loss of capillaries in the DP of the FVB/N retina, i.e., the average vascular area fractions were 26.4 ± 2, 25.6 ± 1.7, and 19.2 ± 1.5 (n = 8) in the wild-type and 4.3 ± 1, 7.3 ± 1.2, and 0 (n = 8) in the FVB/N retina. The results strongly suggest that early-onset photoreceptor degeneration could cause vascular remodeling in the IP and DP of the FVB/N retina at P14.

Early-onset photoreceptor degeneration also influences vascular outgrowth in the IP and DP of the diseased retina. Fig. 4D shows the results of average vascular outgrowth (%) in the SP, IP, and DP of the wild-type and FVB/N retinas. The histogram bars in Fig. 4D show that average vascular outgrowth values (%) in the IP of the wild-type and FVB/N retinas were 39.7 ± 5.5 (n = 8) and 82.2 ± 6 (n = 8), respectively, and the DP of those retinas were 98.2 ± 1.2 (n = 8) and 52.6 ± 8 (n = 8), respectively. The results indicate that vascular outgrowth increased by approximately 48% in the IP and reduced by approximately 54% in the DP of the FVB/N retina. Note that the SPs were well developed in both the wild-type and FVB/N retinas at P14.

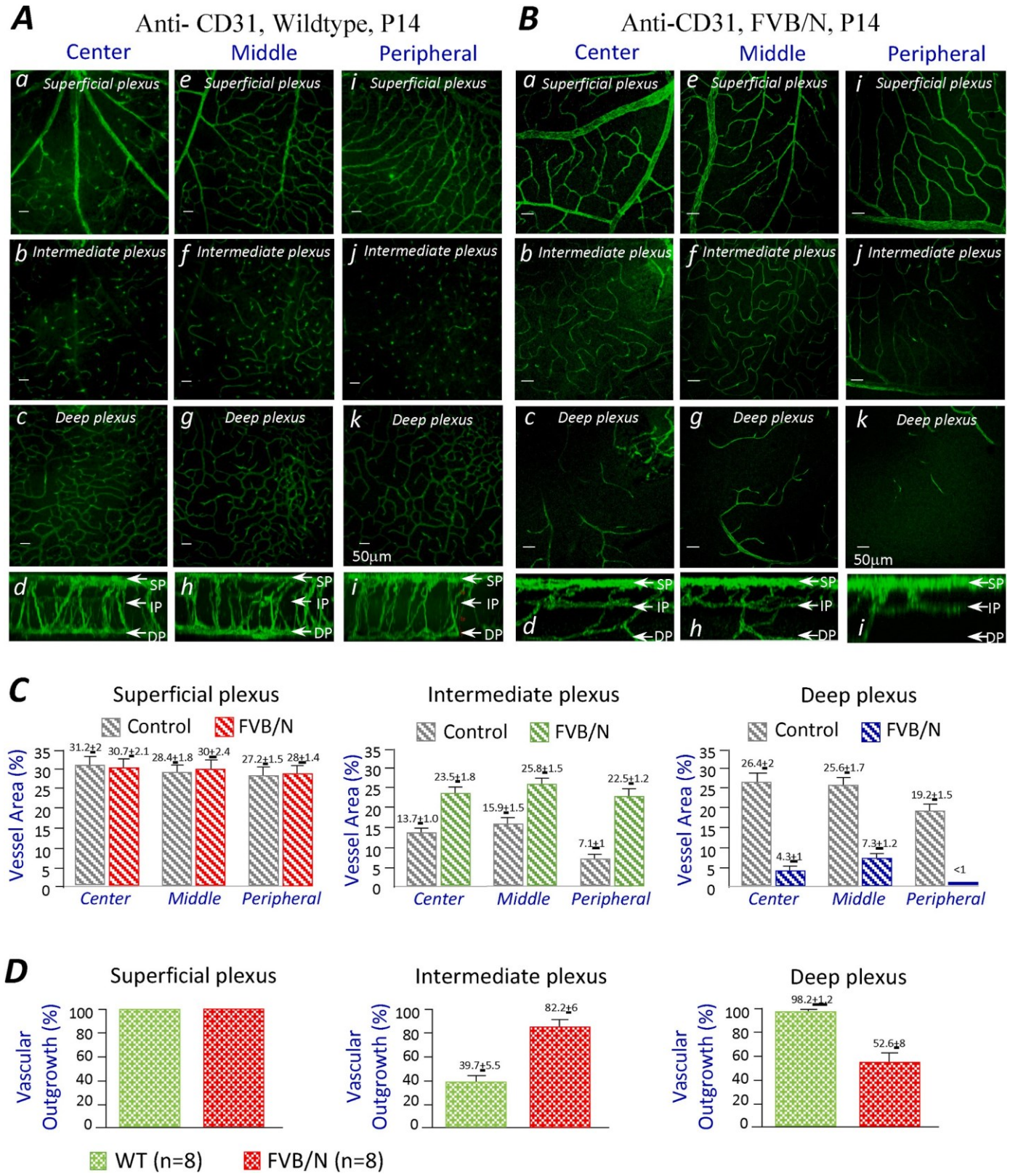

Fig. 4. Vascular development in the wild-type 129SvEv and FVB/N mouse retinas at P14 labeled with anti-CD31. **(A)** Representative images taken in the central, middle, and peripheral areas of the superficial, intermediate, and deep plexus in a whole-mounted wild-type retina (see *a-c, e-g, i-k*); a cross-section of confocal z-stacked images illustrates the trilaminar vascular network (see *d, h, i*). **(B)** Images for each plexus of the age-matched FVB/N retina and a cross-sectional view of the trilaminar network. **(C)** Quantification and comparison of vascular density measured in each plexus of the wild-type and the FVB/N retinas. **(D)** Quantitative analysis of vascular outgrowth in each plexus of the trilaminar network at age P14. **SP**: superficial plexus; **IP**: intermediate plexus; **DP**: deep plexus.

3.6. Abnormal vasculature in the young adult FVB/N mouse retina

At P21, most photoreceptors were degenerated in the FVB/N mice, with only a single layer of photoreceptor nuclei remaining in the ONL (see Fig. 1A). The animals had completely lost their vision. Under these conditions, only a few dilated vessel branches were found in the DP of the FVB/N retina (Fig. 5A*f*). These were branches from the ascending venules in the SP (see the white circles in *d, e, f* in Fig. 5A). No arteriole capillaries were present in the DP, which indicated that there was no oxygenated blood circulation in the DP of the diseased retina. In contrast, the DP of the age-matched wild-type retina was formed of an arteriolar and venular capillary meshwork (Fig. 5A*c*).

Quantitative analyses of the vascular density at each plexus shows that the average vascular area fractions in the DP (central, middle, and periphery) were 30 ± 1.8, 32 ± 2.1 and 31.2 ± 1.5 (n = 10) in the wild-type; however, the values reduced to 2.9 ± 0.7, 4.3 ± 1.3, and 0 (n = 8) in the age-matched FVB/N retina (bottom panel, Fig. 5B). Average vascular area fractions in the IP (central, middle, and periphery) were 23.2 ± 1.2, 24.7 ± 1.8, and 25.4 ± 2 (n = 10) in the wild-type and 19.5 ± 1.6, 20.5 ± 1.8, and 21 ± 1.2 (n = 8) in the FVB/N retina, i.e., there were slight reductions in the IP of the diseased retina (Fig. 5B, middle panel). The analysis data also show that vascular remodeling continued in the IP of the FVB/N retina. There was an approximate 17%, 11%, and 7% loss of vascular densities in the central, middle, and peripheral areas of the IP over the time period of retinal development from P14 to P21.

The loss of photoreceptors had little or no effect on vessel densities of the SP in the FVB/N retina at P21 (Fig. 5B, top panel). Nevertheless, we observed vessel regression in the SP indicated by slight reductions in the vessel area percentages in the central area of both the wild-type and the FVB/N retinas between 14 and P21.

Quantitative assessments of vascular elements: total number of branches, total number of joints, total length of the branches, vascular fraction and outgrowth, in the developing DP of the 129SvEv retinas and FVB/N (rd1) retinas are summarized in Table 1, showing abnormal vascular development in the DP of the rd1 mice at P8, P14 and P21.

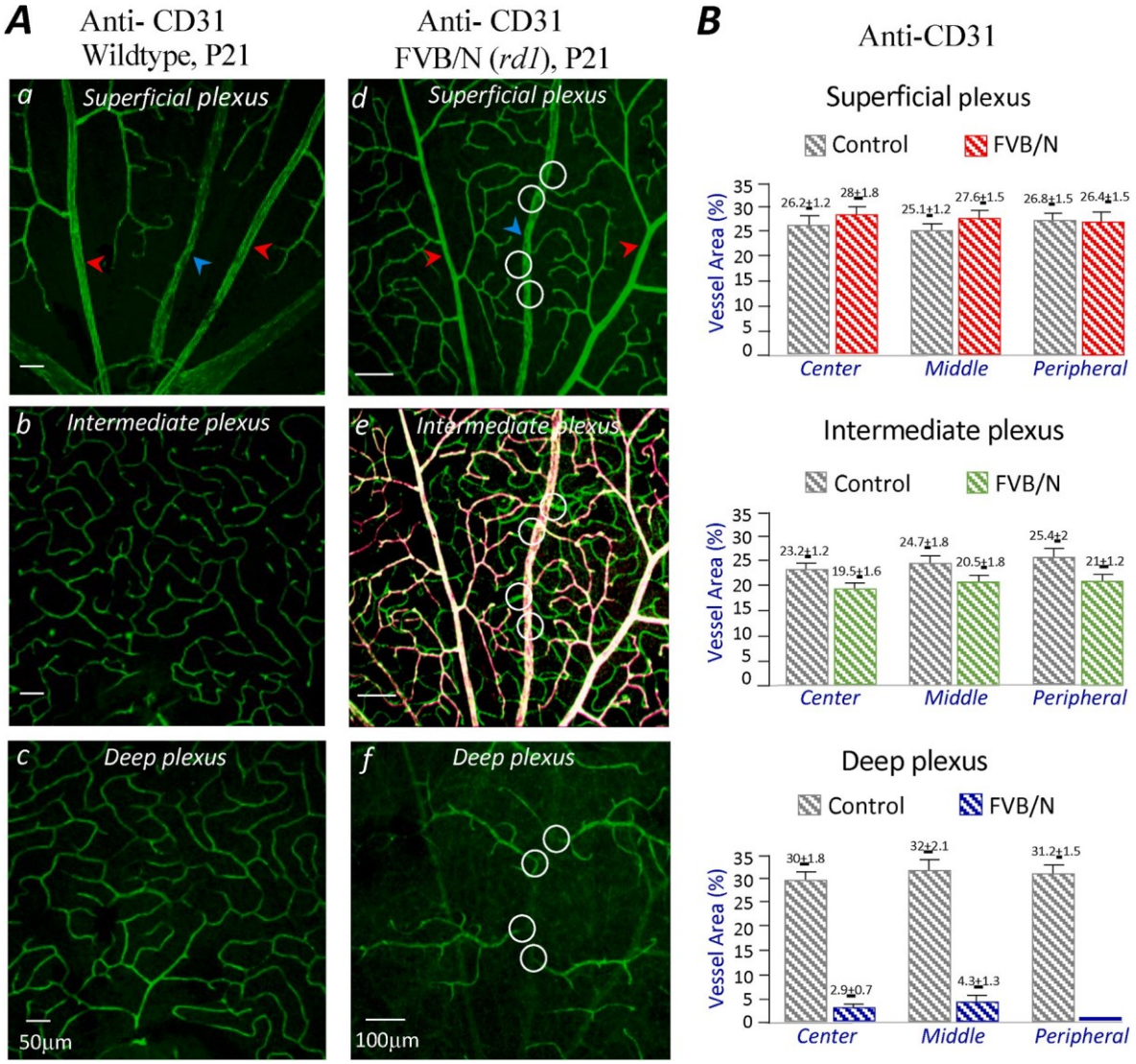

Fig. 5. Representative images of abnormal vascular development in the photoreceptor degenerated retina of the FVB/N mouse at P21. (**A**) Retinal vasculature in the wild-type (*a, b, c*) and FVB/N retinas (*d, e, f*) labeled with anti-CD31. The white circles indicate the vessels in the deep plexus arising from the venules in the superficial plexus. (**B**) Quantification and comparison of vascular area densities in each plexus of the trilaminar network in the wild-type and age-matched FVB/N mouse retina. **Red arrowhead**: arteriole. **Blue arrowhead**: venule. (For interpretation of the references to color in this figure legend, the reader is referred to the Web version of this article.)

Table 1
Summary of vascular branching morphology, density and outgrowth for the deep plexus of the 129SvEv (wildtype control) and FVB/N (rd1) at developing age P8, P14 and P21, illustrating the abnormal development of the deep plexus in the rd1 retinas. Progressive Vascular Degeneration in the Deep Plexus of RD10 Mouse Retina.

P8 (WT) n = 8	Total # of Branches	Total # of Junctions	Total length of Branches (mM)	Area Fraction (%)	Vessel Outgrowth (%)
Center	725 ± 28	363 ± 13	20.5 ± 0.3	15.7 ± 1.8	43.5 ± 5
Middle	769 ± 31	392 ± 15	21.8 ± 0.4	16.1 ± 1.4	
Periphery	135 ± 22	52 ± 9	3.7 ± 0.1	3.4 ± 0.9	
P8 (rd1) n ¼ 12	Total # of Branches	Total # of Junctions	Total length of Branches (mM)	Area Fraction	Vessel Outgrowth
Center	102 ± 11	17 ± 5	3.5 ± 0.05	5.1 ± 1.2	5.3 ± 1
Middle	-	-	-		
Periphery	-	-	-	-	
P14 (WT) n ¼ 8	Total # of Branches	Total # of Junctions	Total length of Branches (mM)	Area Fraction (%)	Vessel Outgrowth (%)
Center	987 ± 26	465 ± 21	22.4 ± 0.4	26.4 ± 2	98.2 ± 1.2
Middle	958 ± 25	440 ± 24	23.2 ± 0.3	25.6 ± 1.7	
Periphery	842 ± 21	405 ± 18	21.3 ± 0.4	19.2 ± 1.5	
P14 (rd1) n ¼ 8	Total # of Branches	Total # of Junctions	Total length of Branches (mM)	Area Fraction	Vessel Outgrowth
Center	112 ± 16	28 ± 7	4.0 ± 0.03	4.3 ± 1	52.6 ± 8
Middle	93 ± 12	36 ± 8	7.7 ± 0.07	7.3 ± 1.2	
Periphery	3 ± 1	2 ± 1	0.8 ± 0.03	<1	
P21 (WT) n ¼ 8	Total # of Branches	Total # of Junctions	Total length of Branches (mM)	Area Fraction (%)	Vessel Outgrowth (%)
Center	1056 ± 34	487 ± 19	23.8 ± 0.4	30 ± 1.8	98.9 ± 0.6
Middle	1062 ± 28	526 ± 21	24.2 ± 0.4	32 ± 2.1	
Periphery	845 ± 29	437 ± 13	23.2 ± 0.4	31.2 ± 1.5	
P21 (rd1) n ¼ 8	Total # of Branches	Total # of Junctions	Total length of Branches (mM)	Area Fraction	Vessel Outgrowth
Center	197 ± 14	57 ± 8	5.1 ± 0.04	2.9 ± 0.7	62.6 ± 4
Middle	148 ± 18	60 ± 8	5.4 ± 0.04	4.3 ± 1.3	
Periphery	-	-	-	-	

3.7. Vascular degeneration in the rd10 mouse retina

The rd10 mouse retinas did not exhibit developmental changes in the vasculature; however, we found that post-developmental vascular degeneration coincided with the time frame of rd10 mice experiencing photoreceptor degeneration. Given the later onset of photoreceptor degeneration in rd10 mice, we observed a relatively normal outer nuclear layer up until at least P23 (see Fig. 1B), at which point the trilaminar vascular development was complete. Confocal imaging results from P28 C57BL/6 control retina and P28 the rd10 retina labeled with anti-CD31 showed a well-developed SP, IP, and DP in the rd10 retina, compared to those of the control retina (Fig. 6A and B). However, vascular degeneration appeared in the DP at P39 (Fig. 6C), i.e., during the time in which photoreceptor degeneration accelerated in the rd10 retina. At P53, only a few vessel branches remained in the DP (Fig. 6D), which led to loss of blood supply in the distal retina at this age. Apparently, the remaining vessel branches in the DP originated from the venules of the SP (see the white circles in Fig. 6D).

To quantitatively analyze the progressive vascular degeneration of the rd10 mouse retinas, we once more measured the vascular area fraction in the central, middle, and peripheral areas of each plexus at P23, P39, and P53, compared to those of the control retina at P28. The results are shown in Fig. 7. The changes in vessel area fractions in the SP were insignificant at P23, P39, and P53 (left panel, Fig. 7). A significant progressive reduction in vascular densities was present the DP of the rd10 retinas (right panel, Fig. 7). The vascular fractions in the DP (central, middle, and peripheral areas) were 26.5 ± 1.4, 28.7 ± 1.8, and 29.8 ± 2 (n = 6) at P23; 22.5 ± 1.5, 24.1 ± 2, and 22.6 ± 2 (n = 8) at P39; 14.3 ± 1.2, 15.8 ± 1.5, and 9.8 ± 1.2 (n = 6) at P53, compared to the values of 26 ± 1.3, 27.1 ± 1.2 and 26.5 ± 1.2 (n = 4) obtained from the control retina at P28, clearly showing that the vessel densities in the DP of the rd10 retina were reduced by at least 45% (central), 42% (middle), and 64% (periphery) at P53 compared to the control. The results also indicate that the most severe vascular degeneration occurred in the periphery of the DP during retinal degeneration progression in the rd10 mice.

The vessel area fractions in the IP (central, middle and peripheral area) were 24 ± 1.7, 24.8 ± 1.6, and 26.1 ± 1.7 (n = 6) at P23; 22 ± 1.5, 25.2 ± 1.2, and 24.4 ± 1.5 (n = 8) at P39; 20 ± 1.2, 19.5 ± 1.5, and 21.7 ± 1.7 (n = 6) at P53; and 24.7 ± 1.5, 25.4 ± 1.327±1.3 (n = 4) in the control retina at P28 129SvEv(middle panel, Fig. 6D), which represented approximate 19% (central), 23% (middle), and 20% (peripheral) reductions over the time period from P23 to P53. The progressive vascular degeneration in the IP appeared to be much less severe as compared to the effects seen in the DP of the rd10 retina.

A detailed analysis of vascular remodeling in the DP of the rd10 mouse retinas is shown in Table 2. Overall, average quantity of branches in the central, middle, and peripheral areas reduced by 47%, 53%, and 63% at P39 and 79%, 88%, and 94% at P53, as compared to the values observed at P23. In addition, the blood vessels in the DP became elongated and less branched from P23 to P53. The data show a progressive loss of the capillary network in the DP of the rd10 retinas.

4. Discussion

In summary, we used a combination of specific antibody labeling and confocal imaging analyses of single vascular plexuses to study retinal vascular development, remodeling, and degeneration in response to photoreceptor loss. This is distinct from the majority of previous studies, which typically rely on histological staining and optical coherence tomography (OCT) imaging methods. Our study offers detailed information about the vasculatures in healthy and diseased retinas, highlighting the remarkable parallelism between photoreceptor cell loss and vascular degeneration. The results provide valuable insights into the nature of the vascular pathological changes that characterize retinal degenerative diseases such as RP. It should be noted that mouse retinas are the ideal choice for researchers studying the pathogenesis of retinal degenerative diseases due to the postnatal development in mice and the large body of genetically altered mouse models (Liu et al., 2016; Chang, 2012; Chang et al., 2013).

4.1. Photoreceptor degeneration influences vascularization in the rd animals

It is known that the microvasculature in the retinal trilaminar network is associated with tissue oxygenation and nutrition and is highly affected under the conditions of retinal diseases (Phillips et al., 2010; Ferna´ndez-Sa´nchez et al., 2018). We confirmed that the development of the SP in the FVB/N mouse retinas is normal even after most of the photoreceptors are lost at p21. This occurrence is also documented in other rd1 mouse and rat retinal degeneration models (Blanks and Johnson, 1986; Pennesi et al., 2008; Ferna´ndez-Sa´nchez et al., 2018). This may, in part, be because the SP branches off the central retinal

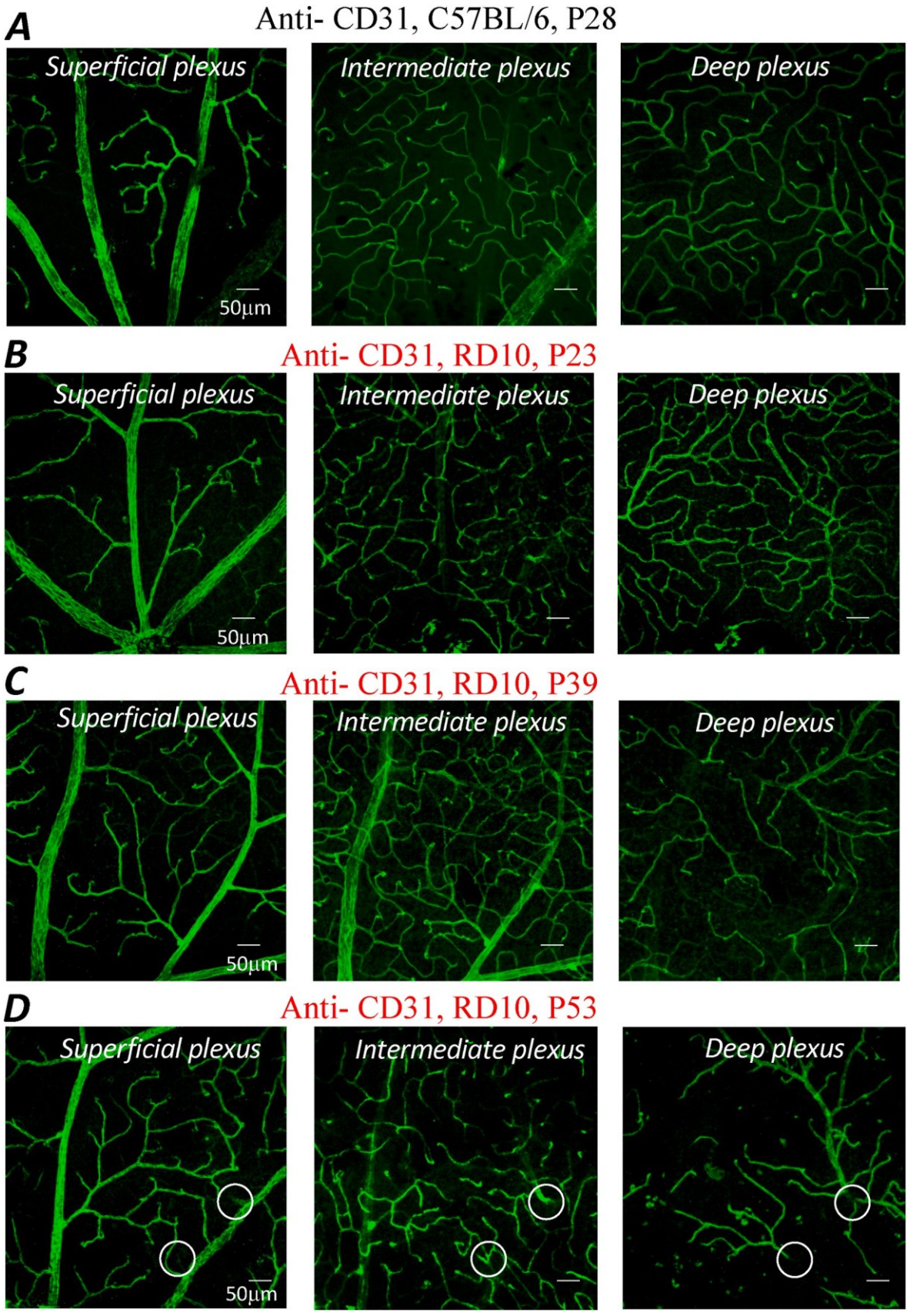

Fig. 6. Representative images of anti-CD31 labeled superficial, intermediate, and deep plexuses of the control retina from C57BL/6 at P28 (**A**) and the rd10 retinas at P23, P39 ad P53, showing progressive vascular degeneration in the retinas of the rd10 mice (**B, C, D**). Loss of capillaries in the deep plexus seen at P39 and P53. The remaining dilated capillaries in the retina at P53 originated from the venules of the superficial plexus (see white circles in **D**).

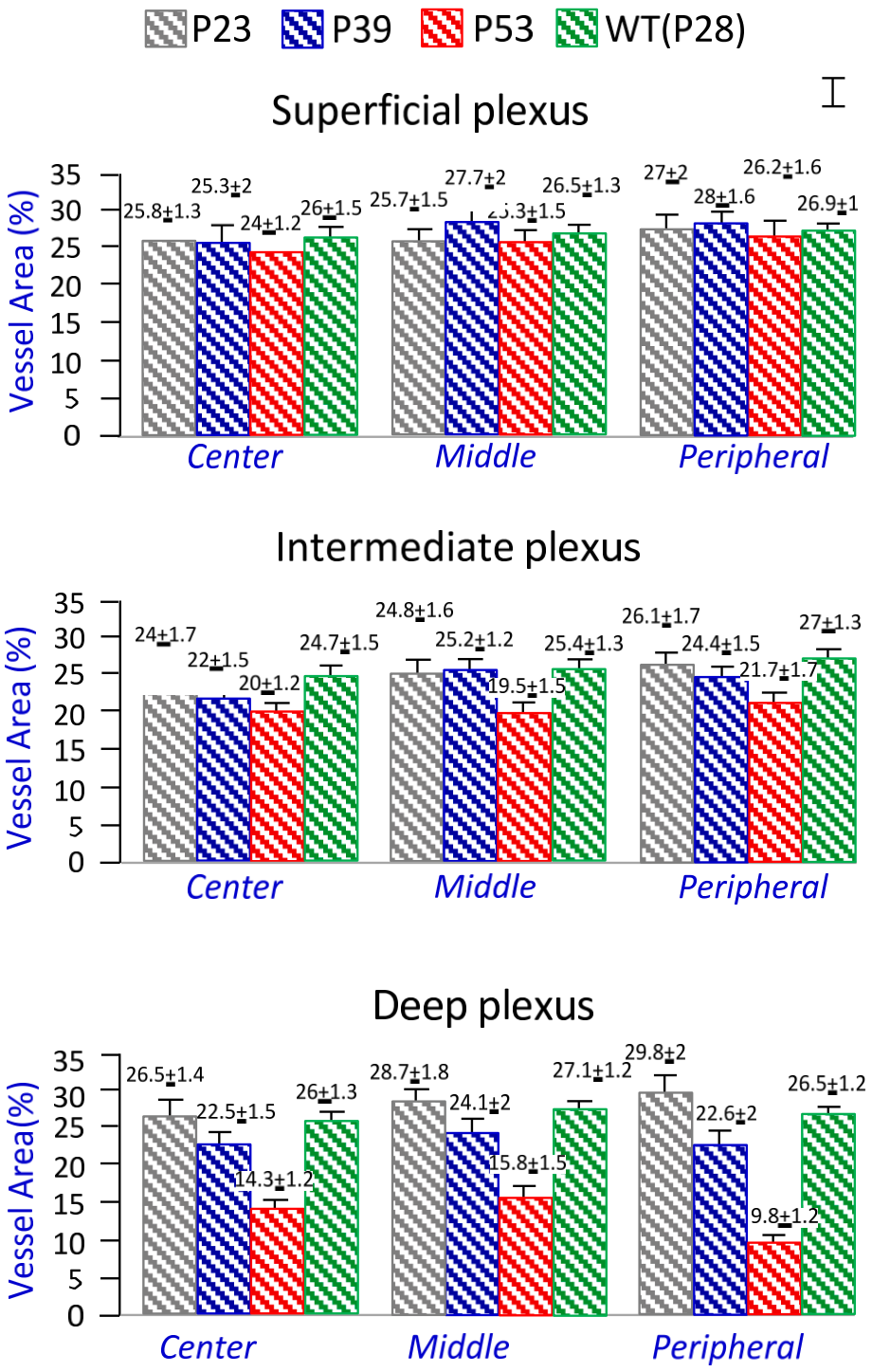

Fig. 7. Quantitative evaluation of vascular densities in the trilaminar network of the rd10 mouse retinas at P23, P39, P53 and C57BL/6 wildtype control retina at P28.

artery and its development occurs prior to significant photoreceptor degeneration. However, early-onset photoreceptor degeneration results in a faster and more severe impact on retinal vascular development in the DP and IP, with the changes being more pronounced in the DP. The results also imply that the distal retina of the rd1 undergoes a hypoxia condition due to the lack of capillary formation in the DP. Interestingly, vascular remodeling in the IP of the rd1 mouse were observed at P14. The capillary growth in the IP seems to be promoted at P14 (see Fig. 4C and D). Possibly, the upregulation of vascular growth in the IP could be a hypoxia-related process that promotes vessel growth by upregulating pre-angiogenic pathways (Krock et al., 2011). By P21, the FVB/N mouse retina was nearly void of all capillary microcirculation in the DP. Our results lead us to conclude that early-onset photoreceptor degeneration disrupts vascular network development in the distal retinas of the diseased mice. These findings may prove especially useful to studies centered on interventions in the developmental stages of the retina.

While the FVB/N mouse retina begins to exhibit vascular degeneration prior to normal development, the rd10 mouse retina can only exhibit vascular degeneration after the development of the vasculature is completed. Given the later onset of photoreceptor degeneration in the

Table 2
Quantitative analysis of morphological changes in vascular branches in the deep plexuses of the C57BL/6 retina at P28 (as a wildtype control) and the rd10 retinas at P23, P39, and P53. The data reflect a progressive loss of capillary branches, junctions, and length of branches in the deep plexuses, corresponding with photoreceptor degeneration in the rd10 retina.

P28, WT (n = 4)	Total # of Branches	Total # of Junctions	Junctions with 3 Branches	Junctions with 5 Branches	Averaged length of longest Branch
Center	1062 ± 32	481 ± 12	458 ± 11	29 ± 7	4.51 ± 0.5
Middle	1087 ± 27	511 ± 9	450 ± 13	34 ± 9	4.8 ± 0.8
Peripheral	788 ± 21	418 ± 8	345 ± 10	20 ± 7	5.1 ± 0.5
P23 (n = 6)	Total # of Branches	Total # of Junctions	Junctions with 3 Branches	Junctions with 5 Branches	Averaged length of longest Branch
Center	1087 ± 25	496 ± 14	450 ± 9	41 ± 5	4.16 ± 0.8
Middle	1108 ± 22	522 ± 15	458 ± 11	46 ± 5	4.28 ± 0.8
Peripheral	807 ± 16	422 ± 8	342 ± 7	28 ± 3	4.6 ± 0.7
P39 (n = 8)	Total # of Branches	Total # of Junctions	Junctions with 3 Branches	Junctions with 5 Branches	Average length of longest Branch
Center	571 ± 28	287 ± 9	258 ± 10	28 ± 4	4.4 ± 0.7
Middle	519 ± 17	276 ± 12	221 ± 7	22 ± 4	4.68 ± 0.8
Peripheral	302 ± 7	142 ± 6	98 ± 5	12 ± 2	4.9 ± 0.5
P53 (n = 6)	Total # of Branches	Total # of Junctions	Junctions with 3 Branches	Junctions with 5 Branches	Average length of longest Branch
Center	230 ± 6	111 ± 4	84 ± 4	7 ± 2	7 ± 0.5
Middle	137 ± 5	52 ± 3	14 ± 3	2 ± 0.4	7.8 ± 0.5
Peripheral	49 ± 3	12 ± 3	7 ± 2	0	8.5 ± 0.3

Quantitative analysis of morphological changes in vascular branches in the deep plexuses of rd10 retinas at P23, P39, and P53. The data reflect a progressive loss of capillary branches, junctions, and length of branches in the deep plexuses, corresponding with photoreceptor degeneration in the rd10 retina.

rd10 mice, we expected to see relatively normal vascular development up until at least p23, at which point the trilaminar plexuses are completely developed. Indeed, vascular degeneration occurred within the time frame during which the rd10 mice experienced photoreceptor degeneration after the fourth postnatal week, as we observed at P39 and P53. Therefore, the rd10 mouse retina serves as an important model for assessing photoreceptor degeneration-caused retinal vascular remodeling in adult animals.

As the primary function of capillaries is the exchange of materials between the blood and tissue cells, retinas have extensive capillary networks because they are highly metabolically active and require an abundant supply of oxygen and nutrients. In the diseased retinas, the arteriovenous capillary networks were initially disrupted in the DP, which then probably extended to the IP as the disease progressed. Oxidative stress and a loss of nutrient supplies in the distal retina would accelerate neurodegeneration in this region.

4.2. Quantitative analyses of the influence of photoreceptor degeneration on retinal vasculature

To quantitatively analyze retinal vasculatures in wild-type and diseased mouse retinas, we utilized the open-source ImageJ analysis software (FIJI) to process the confocal images acquired from each single plexus of the vascular trilaminar network. We chose to use single-plexus analyses and comparisons so as to ensure more accurate measurements of the three-dimensional retinal vasculature. In this manner, we hoped to overcome the limitations of whole retinal tissue analysis (Rust et al., 2019). In addition, we chose biologically relevant parameters, such as vascular area fraction, number of sprouts, vascular outgrowth, number of branches, average length of longest branches, etc., to better characterize and quantitatively analyze the changes in the vascular structure following photoreceptor degeneration in the RP mouse models. As an example, in the study on the rd10 retina, we demonstrate that the retina exhibited normal vascular development until the end of the fifth week, after which it began to lose vascular density in the central, middle, and peripheral areas of the DP, as evidenced by a largely reduced vascular area fraction, a decreased number of branches, and junctions of branches, but an increased average venule of capillary branch length. The degeneration of capillaries in the DP of the rd10 retinas appeared to hinder the formation of junctions but increase the length of the vessel branches. Vascular degeneration is also seen to a much lesser extent in the IP compared to the DP. These findings are consistent with data from studies performed on similar animal models (Blanks and Johnson, 1986; Lahdenranta et al., 2001; Pennesi et al., 2008). The results lead us to conclude that vascular changes are correlated with the onset of photoreceptor degeneration. By systematically characterizing the vascular changes following photoreceptor degeneration in these mouse models using biologically relevant parameters, we offer insights into the time frame of disease processes that are unique to retinal degeneration. Our results support the use of vascular density parameters to quantitatively analyze vascular changes during retinal degenerative conditions. In addition, our statistical analyses provide a scientific basis for imaging data describing vascular remodeling in retinal degenerative diseases.

4.3. Different roles of two endothelial junction-associated proteins in retinal vascular formation

Our results suggest that the two endothelial junction-associated proteins, PECAM1 (CD31) and VE-cadherin (CD144), play different roles in the process of capillary formation during retinal vascular development. CD31 appears to be required for endothelial cell elongation, migration, and/or invasion, and for cell–cell association when forming network structures (Feng et al., 2016; Lertkiatmongkol et al., 2016). Although CD144 also appears to be required for cell–cell association, it additionally plays some role in the process of vascularization or sprouting angiogenesis (Dorrell et al., 2002; Bravi et al., 2014). Therefore, CD144 is arguably one of the most important adhesion molecules for the formation of the retinal trilaminar structure and the stability of their junctions. We found that CD144 expression was suppressed in the DP-forming stage in the FVB/N retina at P8, suggesting that photoreceptor degeneration may somehow influence deep vascular plexus development by inhibiting CD144 expression and, therefore, inhibit vascular development in the distal retina. This supports the idea that CD144 is required for forming vascular networks during retinal development.

It is known that CD144 is expressed specifically in endothelial cells and mediates calcium-dependent adherent junctions between the cells (Suzuki et al., 2017; Lampugnani et al., 1992; Breier et al., 1996). CD144 is also expressed in endothelial precursor cells and in the earliest blood vessels throughout the embryo (Breier et al., 1996). Knockout of the CD144 gene in mouse embryos results in widespread disruption of the initial vascular network and early embryonic lethality (Carmeliet et al., 1999; Gory-Faur´e et al., 1999; Montero-Balaguer et al., 2009). More recent studies have suggested that CD144 is not, in fact, required for the initial assembly of the vascular network, but instead is required for the maintenance of immature vessels (Crosby et al., 2005). This results in early vascular development occurring normally, but the primitive vessels fall apart in the absence of the CD144 protein. Our results agree with those of previous studies showing that a lack of CD144 severely impairs sprouting angiogenesis and vessel regression in the mutants. These observations suggest that CD144 has multiple functions in vascular development.

4.4. Perspectives in the study

This study highlights the remarkable parallelism between photoreceptor cell loss and vascular degeneration. Our results support the notion that photoreceptor survival is a key element for interventions directed at the rescue of retinal vasculature both before and after development. Therefore, attempts at understanding the mechanism of photoreceptor degeneration-caused pathological changes in the retinal vasculature are vital in order to produce successful interventions that mitigate or prevent the progression of retinal degeneration and the subsequent loss of vision. There are potential targets for studying the mechanisms related to vascular function and degeneration. One such avenue of research involves exploring the molecular pathways that modulate oxidative stress and inflammation. In retinal degeneration, there is an imbalance between the pro-oxidant signaling activity that generates reactive oxygen species and antioxidant activity that serves to eliminate them, which can lead to excess oxidative stress and subsequent inflammation. Such conditions would further cause altered expressions of certain genes that modulate vascular formation and endothelial function. Among these, vascular endothelial growth factor (VEGF) and platelet-derived endothelial cell growth factor (PDGF) are two examples of genes that exhibit altered expression under pathological conditions of oxidative stress and inflammation (Alon et al., 1995; Fruttiger et al., 1996; Penn et al., 2000, 2008). Considering that VEGF and PDGF play major roles in the formation of primary vasculature and the subsequent growth and proliferation of vascular endothelial cells, there is a potential avenue of study concerning the actions of molecular pathways involving these growth factors in the photoreceptor degeneration-induced abnormal vasculature. While these studies will likely extend our knowledge of the mechanisms underlying retinal degeneration, it remains an important challenge in treating these diseases. As the vascular system is critical for supplying oxygen and nutrients to tissues, especially those with high metabolic demand as seen in the distal retina, given the correlation between photoreceptor degeneration and changes in the vascular network, approaches to therapies for retinal degenerative diseases must take into account the mechanisms of both events.

Although RP has no cure, treatments are being developed, such as gene therapy, stem cell therapy, and oral medications. Other approaches are being investigated to help reshape the future for those with vision impairment in RP. Understanding the associations between vascular changes in the disease will certainly help RP patients. Therefore, future studies should look into strategies promoting blood vessel survival and protection at specific time points as potential therapies for mitigating retinal degeneration.

This study also aimed to support future endeavors by identifying a practical and consistent method for studying the vascular architecture via three-dimensional models in conjunction with a quantitative analysis of vascular changes that can be reproduced and compared across studies in an efficient manner. The readily available open-source imaging software coupled with easily accessible analytical plug-ins resulting from collaborations across disciplines have also contributed to our understanding of vascular changes in retinal degenerative disease. As the retina is an extension of the neural network of the brain and shares many similar pathophysiological changes and mechanisms of actions with the brain, studies carried out in mouse retinas have a broad impact in this area.

Declarations of interest

None.

Data availability

Data will be made available on request.

Acknowledgements

This work was supported by a Pilot Award, Brain Institute at Florida Atlantic University (W.S.); National Eye Institute, EY14161 (W.S.) and National Science Foundation, IOS-2126141 and IOS-1021646 (W.S.).

References

Alon, T., Hemo, I., Itin, A., Pe'er, J., Stone, J., Keshet, E., 1995. Vascular endothelial growth factor acts as a survival factor for newly formed retinal vessels and has implications for retinopathy of prematurity. Nat. Med. 1, 1024–1028. https://doi.org/10.1038/nm1095-1024.

Barhoum, R., Martinez-Navarrete, G., Corrochano, S., Germain, F., Fern´andez-S´anchez, L., de la Rosa, E.J., de la Villa, P., Cuenca, N., 2008. Functional and structural modifications during retinal degeneration in the *rd10* mouse. Neuroscience 155 (3), 698–713.

Blanks, J.C., Johnson, L.V., 1986. Vascular atrophy in the retinal degenerative rd mouse. J. Comp. Neurol. 254, 543–553 [PubMed: 3805362].

Bowes, C., Li, T., Danciger, M., Baxter, L.C., Applebury, M.L., Farber, D.B., 1990. Retinal degeneration in the rd mouse is caused by theβ-subunit of rod cGMP-phosphodiesterase. Nature 347, 677–680. PMID: 1977087.

Bravi, L., Dejana, E., Lampugnani, M.G., 2014. VE-cadherin at a glance. Cell Tissue Res. 355, 515–522. https://doi.org/10.1007/s00441-014-1843-7.

Breier, G., Breviario, F., Caveda, L., Berthier, R., Schnürch, H., Gotsch, U., Vestweber, D., Risau, W., Dejana, E., 1996. Molecular cloning and expression of murine vascular endothelial-cadherin in early stage development of cardiovascular system. Blood 87 (2), 630–641. PMID: 8555485.

Carmeliet, P., Lampugnani, M.G., Moons, L., Breviario, F., Compernolle, V., Bono, F., Balconi, G., Spagnuolo, R., Oosthuyse, B., Dewerchin, M., Zanetti, A., Angellilo, A., Mattot, V., Nuyens, D., Lutgens, E., Clotman, F., de Ruiter, z M.C., Gittenberger-de Groot, A., Poelmann, R., Lupu, F., Herbert, J.M., Collen, D., Dejana, E., 1999. Targeted deficiency or cytosolic truncation of the VE-cadherin gene in mice impairs VEGF-mediated endothelial survival and angiogenesis. Cell 98, 147–157. https://doi.org/10.1016/s0092-8674(00)81010-7.

Carter-Dawson, L.D., LaVail, M.M., Sidman, R.L., 1978. Differential effect of the rd mutation on rods and cones in the mouse retina. Invest. Ophthalmol. Vis. Sci. 17, 489–498.

Chang, B., 2012. Mouse models for studies of retinal degeneration and diseases. In: Retinal Degeneration. Humana Press, Totowa, NJ, pp. 27–39.

Chang, B., Hawes, N.L., Hurd, R.E., Davisson, M.T., 2002. Nusinowitz S, Heckenlively JR. Retinal degeneration mutants in the mouse. Vis. Res. 42 (4), 517–525. PMID: 11853768.

Chang, B., Hawes, N.L., Pardue, M.T., German, A.M., Hurd, R.E., Davisson, M.T., Nusinowitz, S., Rengarajan, K., Boyd, A.P., Sidney, S.S., Phillips, M.J., Stewart, R.E., Chaudhury, R., Nickerson, J.M., Heckenlively, J.R., Boatright, J.H., 2007. Two mouse retinal degenerations caused by missense mutations in the beta-subunit of rod cGMP phosphodiesterase gene. Vision Res. 47, 624–633. https://doi.org/10.1016/j.visres.2006.11.020.

Chang, B., Hurd, R., Wang, J., Nishina, P., 2013. Survey of common eye diseases in laboratory mouse strains. Invest. Ophthalmol. Vis. Sci. 54, 4974–4981. https://doi.org/10.1167/iovs.13-12289.

Chen, J., Liu, C.H., Sapieha, P., 2016. Retinal vascular development. In: Stahl, A. (Ed.), Anti-Angiogenic Therapy in Ophthalmology. Essentials in Ophthalmology. Springer, Cham. https://doi.org/10.1007/978-3-319-24097-8_1.

Cronin, T., Lyubarsky, A., Bennett, J., 2012. Dark-rearing the rd10 mouse: implications for therapy. Adv. Exp. Med. Biol. 723, 129–136. https://doi.org/10.1007/978-1-4614-0631-0_18.

Crosby, C.V., Fleming, P.A., Argraves, W.S., Corada, M., Zanetta, L., Dejana, E., Drake, C. J., 2005. VE-cadherin is not required for the formation of nascent blood vessels but acts to prevent their disassembly. Blood 105 (7), 2771–2776. https://doi.org/10.1182/blood-2004-06-2244, 2005.

Dimaio, T.A., Wang, S., Huang, Q., Scheef, E.A., Sorenson, C.M., Sheibani, N., 2008. Attenuation of retinal vascular development and neovascularization in PECAM-1 deficient mice. Dev. Biol. 315 (1), 72–88. https://doi.org/10.1016/j.ydbio.2007.12.008.

Dorrell, M.I., Aguilar, E., Friedlander, M., 2002. Retinal vascular development is mediated by endothelial filopodia, a Preexisting Astrocytic Template and Specific R-Cadherin Adhesion. Invest. Ophthalmol. Vis. Sci. 43 (11), 3500–3510. PMID: 12407162.

Feng, Y.M., Chen, X.H., Zhang, X., 2016. Roles of PECAM-1 in cell function and disease progression. Eur. Rev. Med. Pharmacol. Sci. 20, 4082–4088. PMID: 27775789.

Fern´andez-S´anchez, L., Esquiva, G., Pinilla, I., Lax, P., Cuenca, N., 2018. Retinal vascular degeneration in the transgenic P23H rat model of retinitis pigmentosa. Front. Neuroanat. 12 https://doi.org/10.3389/fnana.2018.00055, 29.

Fruttiger, M., Calver, A.R., Krüger, W.H., Mudhar, H.S., Michalovich, D., Takakura, N., Nishikawa, S., Richardson, W.D., 1996. PDGF mediates a neuron-astrocyte interaction in the developing retina. Neuron 17, 1117–1131. https://doi.org/10.1016/s0896-6273(00)80244-5.

Gimenez, E., Montoliu, L., 2001. A simple chain reaction assay for genotyping the retinal degeneration mutation (Pdebrd1) in FVB/N-derived transgenic mice. Lab. Anim 35, 153–156. https://doi.org/10.1258/0023677011911525.

Gory-Faur´e, S., Prandini, M.H., Pointu, H., Roullot, V., Pignot-Paintrand, I., Vernet, M., Huber, P., 1999. Role of vascular endothelial-cadherin in vascular morphogenesis. Development 126 (10), 2093–2102. https://doi.org/10.1242/dev.126.10.2093.

Ivanova, E., Toychiev, A.H., Yee, C.W., Sagdullaev, B.T., 2014. Intersublaminar vascular plexus: the correlation of retinal blood vessels with functional sublaminae of the inner plexiform layer. Invest. Ophthalmol. Vis. Sci. 55 (1), 78–86. https://doi.org/10.1167/iovs.13-13196.

Krock, B.L., Skuli, N., Simon, M.C., 2011. Hypoxia-induced angiogenesis: good and evil. Genes Cancer 2 (12), 1117–1133. https://doi.org/10.1177/1947601911423654.

Lahdenranta, J., Pasqualini, R., Schlingemann, R.O., Hagedorn, M., Stallcup, W.B., Bucana, C.D., Sidman, R.L., Arap, W., 2001. An anti-angiogenic state in mice and humans with retinal photoreceptor cell degeneration. Proc. Natl. Acad. Sci. USA 98, 10368–10373. https://doi.org/10.1073/pnas.181329198.

Lampugnani, M.G., Resnati, M., Raiteri, M., Pigott, R., Pisacane, A., Houen, G., Ruco, L. P., Dejana, E., 1992. A novel endothelial-specific membrane protein is a marker of cell-cell contacts. J. Cell Biol. 118, 1511–1522. https://doi.org/10.1083/jcb.118.6.1511.

Lertkiatmongkol, P., Liao, D., Mei, H., Hu, Y., Newman, P.J., 2016. Endothelial functions of PECAM-1 (CD31). Curr. Opin. Hematol. 23 (3), 253–259. https://doi.org/10.1097/MOH.0000000000000239.

Li, B., Gografe, S., Munchow, A., Lopez-Toledano, M., Pan, Z.H., Shen, W., 2019. Sex-related differences in the progressive retinal degeneration of the rd10 mouse. Exp. Eye Res. 187, 107773 https://doi.org/10.1016/j.exer.2019.107773.

Liu, H., Tang, J., Du, Y., Saadane, A., Tonade, D., Samuels, I., Veenstra, A., Palczewski, K., Kern, T.S., 2016. Photoreceptor cells influence retinal vascular degeneration in mouse models of retinal degeneration and diabetes. Invest. Ophthalmol. Vis. Sci. 57 (10), 4272–4281. https://doi.org/10.1167/iovs.16-19415.

Milde, F., Lauw, S., Koumoutsakos, P., Iruela-Arispe, M.L., 2013. The mouse retina in 3D: quantification of vascular growth and remodeling. Integr. Biol. 5 (12), 1426–1438. https://doi.org/10.1039/c3ib40085a.

Montero-Balaguer, M., Swirsding, K., Orsenigo, F., Cotelli, F., Mione, M., Dejana, E., 2009. Stable vascular connections and remodeling require full expression of VE-cadherin in zebrafish embryos. PLoS One 4 (6), e5772. https://doi.org/10.1371/journal.pone.0005772.

Pang, J., Boye, S.L., Kumar, A., et al., 2008. AAV-mediated gene therapy for retinal degeneration in the rd10 mouse containing a recessive PDEbeta mutation. Invest. Ophthalmol. Vis. Sci. 49, 4278–4283. PubMed: 18586879.

Pennesi, M.E., Nishikawa, S., Matthes, M.T., Yasumura, D., LaVail, M.M., 2008. The relationship of photoreceptor degeneration to retinal vascular development and loss in mutant rhodopsin transgenic and RCS rats. Exp. Eye Res. 87 (6), 561–570. https://doi.org/10.1016/j.exer.2008.09.004.

Penn, J.S., Li, S., Naash, M.I., 2000. Ambient hypoxia reverses retinal vascular attenuation in a transgenic mouse model of autosomal dominant retinitis pigmentosa. Invest. Ophthalmol. Vis. Sci. 41, 4007–4013.

Penn, J.S., Madan, A., Caldwell, R.B., Bartoli, M., Caldwell, R.W., Hartnett, M.E., 2008. Vascular endothelial growth factor in eye disease. Prog. Retin. Eye Res. 27 (4), 331–371. https://doi.org/10.1016/j.preteyeres.2008.05.001.

Phillips, M.J., Otteson, D.C., Sherry, D.M., 2010. Progression of neuronal and synaptic remodeling in the rd10mouse model of retinitis pigmentosa. J. Comp. Neurol. 518 (11), 2071–2089. https://doi.org/10.1002/cne.22322.

Rust, R., Gro¨nnert, L., Dogançay, B., Schwab, M.E., 2019. A revised view on growth and remodeling in the retinal vasculature. Sci. Rep. 9, 3263. https://doi.org/10.1038/s41598-019-40135-2.

Selvam, S., Kumar, T., Fruttiger, M., 2018. Retinal vasculature development in health and disease. Prog. Retin. Eye Res. 63, 1–19. https://doi.org/10.1016/j.preteyeres.2017.11.001.

Sun, Y., Smith, L.E.H., 2018. Retinal vasculature in development and diseases. Annu Rev Vis Sci 4, 101–122. https://doi.org/10.1146/annurev-vision-091517-034018.

Suzuki, S., Sano, K., Tanihara, H., 2017. Diversity of the cadherin family: evidence for eight new cadherins in nervous tissue. Cell Regul. 2, 261–270. https://doi.org/10.1091/mbc.2.4.261.

Yang, J., Nan, C., Ripps, H., Shen, W., 2015. Destructive changes in the neuronal structure of the FVB/N mouse retina. PLoS One 10 (6), e0129719. https://doi.org/10.1371/journal.pone.0129719.